

Numerical Simulation on the Combustion Characteristic of GO_2/GCH_4 Splash Platelet Injector

Yin Liang and Liu Weiqiang

Science and Technology on Scramjet Laboratory, National University of Defense Technology, Changsha, Hunan 410073, People's Republic of China

yl88222@126.com

Abstract. The platelet injector flow is quite different from other injectors due to the platelet technology and complex injection method. This work is aimed at assessing the effect of characteristic chamber length and middle-plate thickness for single-element splash platelet injector. Numerical simulation was adopted to investigate the gaseous methane and gaseous oxygen flow and combustion characteristics. Both characteristic velocity and combustion efficiency are examined for injector design. The results indicate that, with a 0.6mm middle-plate thickness the injector can reach the maximum combustion efficiency and shortest combustion length, but the differences are not obvious for all cases. The characteristic chamber length can be shortened effectively by using splash platelet injector.

1. Introduction

Platelet technology has been identified as a promising technology since 1964, which provides solutions to difficult thermal and fluid flow problems [1]. It has been used to produce heat exchangers, hypersonic leading edge, platelet injector, platelet mixer, micro structured reactor, and other applications [2-5]. Platelet injector is a new type of liquid rocket injector designed by Aerojet in the 1970s. It was widely used in low thrust attitude control engine because of several unique features including excellent response, simple structure, potential high performance with reduced chamber lengths [6,7].

Over the past several decades, considerable efforts have been dedicated to model in platelet injector to understand and predict the flow, mixing and combustion characteristic, many experiences have been accumulated in experiment and technology. Platelet injector exhibits many differences from traditional injector such as atomization characteristic, flow characteristic, design method, combustion stability, and the performance analysis of platelet injector is only limited to experimental analysis, the theoretical analysis is still in blank.

The effect of main configuration parameters, such as spray angle and relative thickness, expending angle have been studied, flow coefficient and mixing efficiency factor were obtained mainly by experiments [8]. Six fundamentally different injection elements were conceived and tested by Aerojet Liquid Rocket Company (ALRC), as a result of the unielement testing; splash platelet injector has proved to be the most promising candidate element with a higher performance, excellent compatibility, and insensitivity to propellant temperature [9,10]. Fanpei Lei et al. investigated the atomizing and mixing characteristics of splash platelet injector with a typical triangular lumen, the results showed that, flow coefficient and mixing efficiency factor increase firstly and then decrease with the increase



of expending angle [11]. Zhihui Guo et al. analyzed the atomization process and special spray feature of splash platelet injector using Particle Dynamics Analyzer (PDA) by experimental study [12]. These series of experiment results suggest that the injector geometry could be optimized in order to achieve a good mixing and combustion characteristics. Numerical simulation holds great, largely unfulfilled promise to be able to meet these requirements. This study is focused on obtaining baseline performance statistics of a gas-gas splash platelet injector which will be a reference for the future injector designs.

2. Numerical methods and Models

2.1. Numerical methods

2.1.1. Governing Equations Time iterative methods are employed for solving the gas-gas combustion field; the governing equations were discretized by control volume integration method.

$$\frac{d}{dt}(\rho\phi V)_{P_0} + a_0\phi_{P_0} = \sum_{j=1}^N a_j\phi_{P_j} + b_0 \quad (1)$$

For the steady-state process, $\frac{d}{dt}(\rho\phi V)_{P_0} = 0$. Here, P_0 is the node of the control volume, P_j is peripheral node, V is control volume, j is subscript of the interface of the control volume, N the number of interface, a_0 and a_j are the operators coefficients for P_0 and P_j , b_0 is the source term of the discrete equation.

2.1.2. Turbulence Model A compressible $\kappa-\varepsilon$ was used for the turbulence model. The turbulence kinetic energy, κ , and its rate of dissipation, ε , are obtained from the following transport equations:

$$\frac{\partial(\rho k)}{\partial t} + \frac{\partial(\rho k u_i)}{\partial x_i} = \frac{\partial}{\partial x_j} \left[\left(\mu + \frac{\mu_t}{\sigma_k} \right) \frac{\partial k}{\partial x_j} \right] + G_k - \rho \varepsilon \quad (2)$$

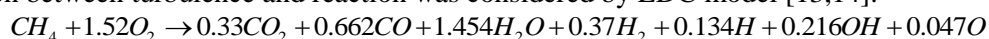
$$\frac{\partial(\rho \varepsilon)}{\partial t} + \frac{\partial(\rho \varepsilon u_i)}{\partial x_i} = \frac{\partial}{\partial x_j} \left[\left(\mu + \frac{\mu_t}{\sigma_\varepsilon} \right) \frac{\partial \varepsilon}{\partial x_j} \right] + C_{1\varepsilon} \frac{\varepsilon}{k} G_k - C_{2\varepsilon} \rho \frac{\varepsilon^2}{k} \quad (3)$$

The turbulent viscosity, μ_t , is computed by combining κ and ε as follows:

$$\mu_t = \rho C_\mu \frac{\kappa^2}{\varepsilon} \quad (4)$$

where, $C_{1\varepsilon} = 1.44$, $C_{2\varepsilon} = 1.44$, $C_\mu = 0.09$, $\sigma_k = 1.0$, $\sigma_\varepsilon = 1.3$

2.1.3 Chemical kinetics model. The CFD code used for calculating the combusting flow field solves the fluid dynamic N-S equations incorporating a compressible $\kappa-\varepsilon$ turbulence model, the chemical kinetics model was calculated by a 9-specie, 1-reaction GO_2 / GCH_4 , which can be seen as follow. The interaction between turbulence and reaction was considered by EDC model [13,14].



2.2 Geometric Model

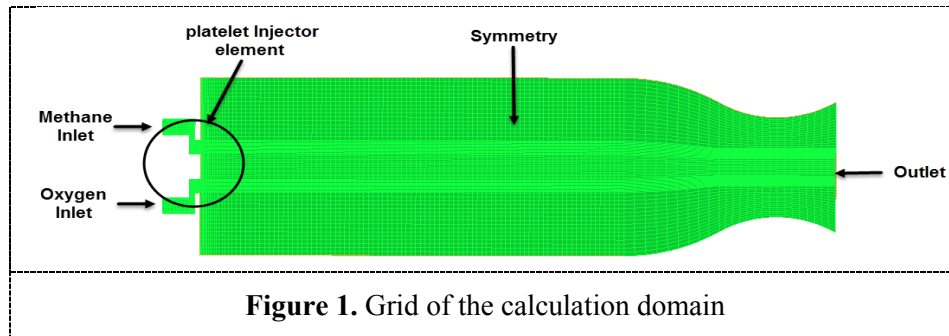


Figure 1. Grid of the calculation domain

Figure 1 shows the grid of the calculation domain, which contains domains of the platelet injector element, symmetry plane, combustion chamber, propellant inlets and pressure outlet. The inlets of methane and oxygen were both fixed mass flow rate, and the inlet turbulence intensities were both set to be 5%. The inlet temperatures are taken as 300 K. The nozzle exit was specified as a supersonic outlet, adiabatic nonslip wall boundaries are enforced at the chamber walls [15, 16]. The parameters of the splash platelet injector and the chamber can be seen in table 1.

Table 1. The parameters of chamber

Parameters	Values
Chamber pressure/MPa	0.85
Mixture Ratio(O/F)	3.2
Mass flow rate /(g/s)	5.5
Inlet gas temperature/K	298.15
Chamber diameter /mm	8.6
Throat diameter /mm	3.84
Theoretical characteristic velocity /m/s	1833.9
Ground Specific impulse /m/s	2270.2

Figure 2 shows the schematic diagram of the splash platelet injector. The key parameters which may control the flow and combustion process may contain: oxidizer orifice (D_o), fuel orifice (D_f), nozzle space (D), expending angle (γ), length of trapezoidal orifice (L_1), thickness of middle-plate ($H2$) and faceplate ($H3$). In this work the length of triangular lumen (L) was fixed to be 1.5mm. Individual middle platelet thickness can range from as thin as 0.3 mm to 1.2 mm. The detail values can be seen in table 2.

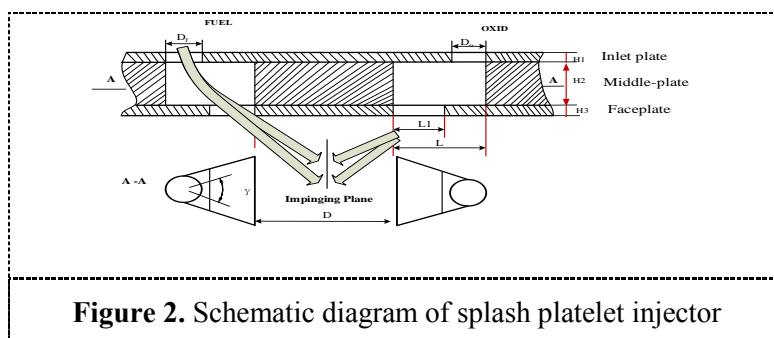


Figure 2. Schematic diagram of splash platelet injector

Table 2. Design parameters of the splash platelet element

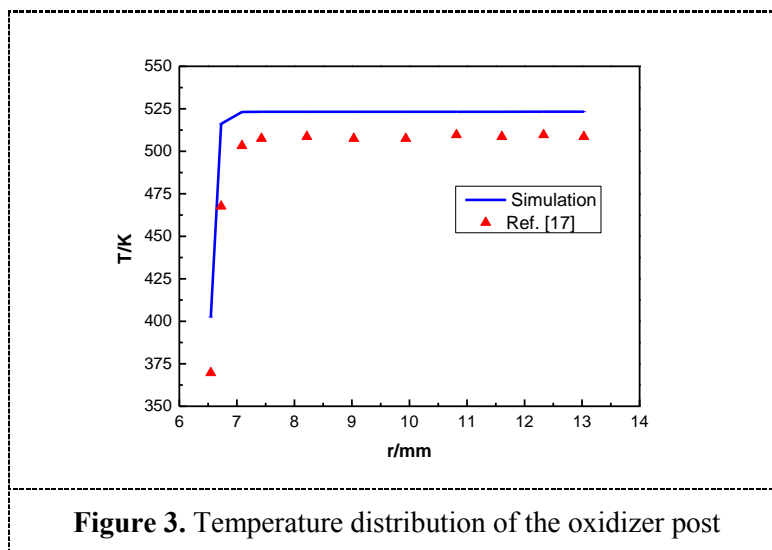
Parameters	H_3/mm	D_O/mm	D_f/mm	D/mm	L/mm	L_1/mm	γ
Values	0.3	1	1	1.2	1.5	0.75	60°

3. Validation of numerical methods

Table 3. Design parameters of the splash platelet element

Propellant	$m/(g/s)$	MR	P_c/MPa	D_c/mm	D_t/m	L^*/mm	R_v
GCH ₄ /GO ₂	5.5	3.5	3	26	14.8	1180	1.77

To demonstrate the validity of numerical methods and chemical kinetics model, simulation was performed on a shear-coaxial GO₂/GCH₄ injector, where P_c is the chamber pressure, MR is mixture ratio, D_c is chamber diameter, D_t is throat diameter, L^* is the characteristic length, R_v is the velocity ratio. Parameters of the shear-coaxial injector are listed in table 3, and the detail design values can get from Ref. [17]. Figure 3 shows the temperature distribution of the oxidizer post, which is consistent with the Ref. data; it can exactly describe the temperature distribution although there is little difference. This testified the accuracy of numerical methods and chemical kinetics model. Detailed chemical reaction model should be adopted in the future works.

**Figure 3.** Temperature distribution of the oxidizer post

4. Results and discussion

4.1 Effect of the characteristic chamber length on characteristic velocity

Characteristic chamber length has an important effect on combustion efficiency. With the characteristic chamber length increasing, the volume and weight of the thrust chamber will be increased, and the surface area and thermal resistance will also be increased. For defining the GO₂/GCH₄ platelet injector thrust chamber length, the design methodology of traditional coaxial injector cannot be directly applied to platelet injector. For the GO₂/GCH₄ platelet injector, there is no mature engine type, so it is always rely on the similar experience of propellant and engine size. Four different characteristic chamber lengths L^* with 300mm, 400mm, 500mm, 600mm were

simulated by Hongyan et al. These results show that when $L^* = 600\text{mm}$, which offer the maximum combustion efficiency and minimum heat load of the chamber wall. Gao Yushan et al. studied the effect of characteristic chamber length of a coaxial injector, the results show that under the same condition the characteristic chamber length of GO_2/GCH_4 is about 1.5 times that of GO_2/GH_2 [17].

Splash platelet injector is the most commonly used injectors, the splash injector involved mechanical atomization of the two propellants by means of direct impingement on the lip of the injection cup and subsequent impingement of the resulting unlike propellant fans [18]. The reason we select the splash platelet injector including ease of manufacture and high performance with reduced chamber length. In this paper, characteristic chamber length $L^* = 300\text{mm}$, 400mm , 500mm , 600mm , 700mm have been chosen for the simulation.

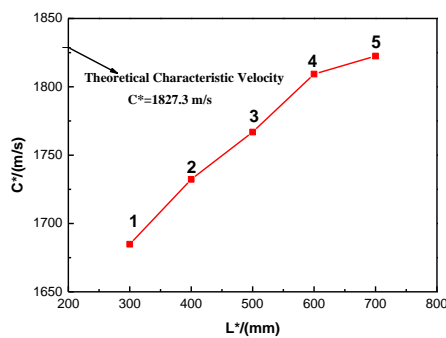


Figure 4. Characteristic velocity vs characteristic chamber length

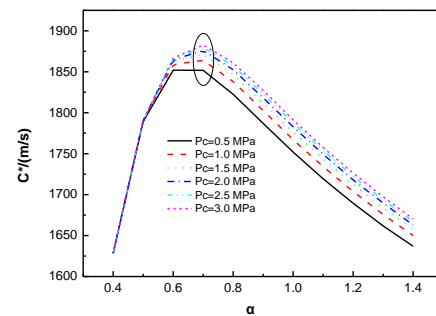


Figure 5. Characteristic velocity vs excess oxidizer coefficient, chamber pressure

Figure 4 shows the effect of characteristic chamber length on characteristic velocity. For $L^* = 300\text{mm}$, the value of characteristic velocity is about 1823.7m/s , indicating that the characteristic velocity efficiency of GO_2/GCH_4 platelet injector can reach 92.2% when characteristic chamber length is about 300mm. With the increase of characteristic chamber length, the characteristic velocity efficiency increased significantly; when $L^* = 600\text{mm}$, characteristic velocity efficiency can reach above 99%, the corresponding values of chamber length is about 120mm. The value of $L^* = 600\text{mm}$ will be adopted in the next simulations. Figure 5 shows that, the characteristic velocity can be improved by applying a high pressure. And there is a parabola relation between characteristic velocity and excess oxidizer coefficient. In this paper, excess oxidizer coefficient $\alpha = 0.8$ has been used for the thermodynamic calculation.

4.2 Temperature

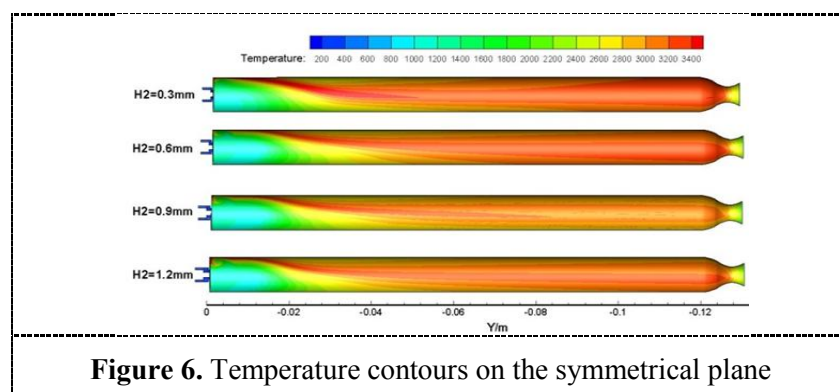


Figure 6. Temperature contours on the symmetrical plane

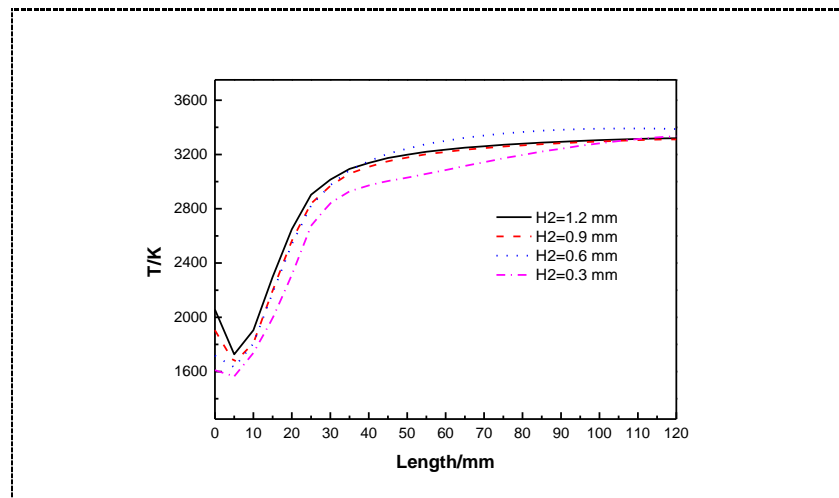


Figure 7. Axial distribution of the chamber wall temperature

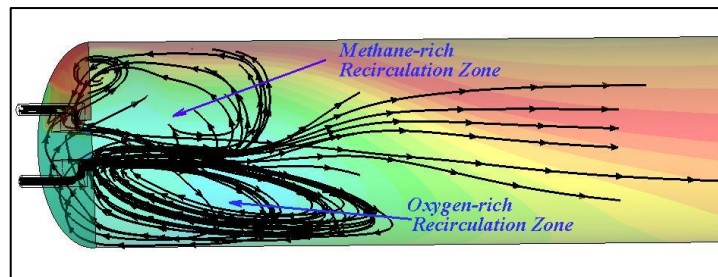


Figure 8. A 3D view of the streamline near faceplate with $H_2=0.3\text{mm}$

When studying the effect of design parameters of the platelet injector on the combustion characteristic, the main results include temperature field, component distribution and combustion efficiency. The walls were modeled with no slip adiabatic wall boundary condition in this simulation, so are unlikely to represent the true value of wall temperature, but the methodology adopted in quantitative analysis can be helpful for this research.

The temperature contours for different middle plate thickness are shown in Figure 6, which serve as a reasonably marker for the GO_2/GCH_4 combust reaction temperature, the result shows that the maximum temperature is about 3400K, very close to the theoretical value, and the temperature contours for all cases indicate an apparent similarity. Non-uniformity combustion is found in the recirculation zones, which comes mainly from the non-uniformity of the velocity distribution. The average axial distribution of the chamber wall temperature are shown in Figure 7, the impinging plane operates a lower temperature than the faceplate area because of incomplete burning, and there is a slight difference between the four cases. When $H_2=0.6\text{mm}$, which operate a higher temperature compared to other cases.

On the other hand, two big scale oxygen-rich and methane-rich recirculation zones are produced near the injector face (see Figure 8), these recirculation zones enhanced mixing and combustion, but can cause a heat flux peak on the faceplate. However, it also serves as a flame holder. These works will be studied in the future.

4.3 Composition distribution

When the excess oxidizer coefficient was set as $\alpha=0.8$, and the specific products only take CO_2 , CO , H_2O , O , H , OH , H_2 . By analysing the thermal calculation, the percentage of mole fraction of CO_2 , CO ,

H₂O was 10.96%, 19.23%, 43.82% respectively, the closer the values approximate to thermal calculation, the more complete combustion has been done. The influence of middle-plate thickness H_2 on percentage of mole fraction of CO₂, CO, H₂O are shown in Figure 9. It can be seen that with the value of H_2 increases, the percentage of the mole fraction of main products increase first and then decrease and finally reach a balance at the position about 40mm away from the faceplate. The concentration of oxygen near the oxidizer post is higher than the fuel post because of different velocity ratio, which can induce to incomplete combustion and efficiency decline.

For methane combustion, the proportion of water was larger than other products, so we can reveal the main combustion area and combustion length by analysing the mole fraction of H₂O. Here we define the combustion length L_c when the mole fraction of water was 90% of the theoretical values. Figure 9 (a) shows the mole fraction of H₂O and the combustion length. This result indicates that larger H_2 is beneficial to promote the combustion performance and reduce combustion length, although its influence is not obvious. In general, for $H_2 = 0.6\text{mm}$, it has better combustion performance, shorter combustion length.

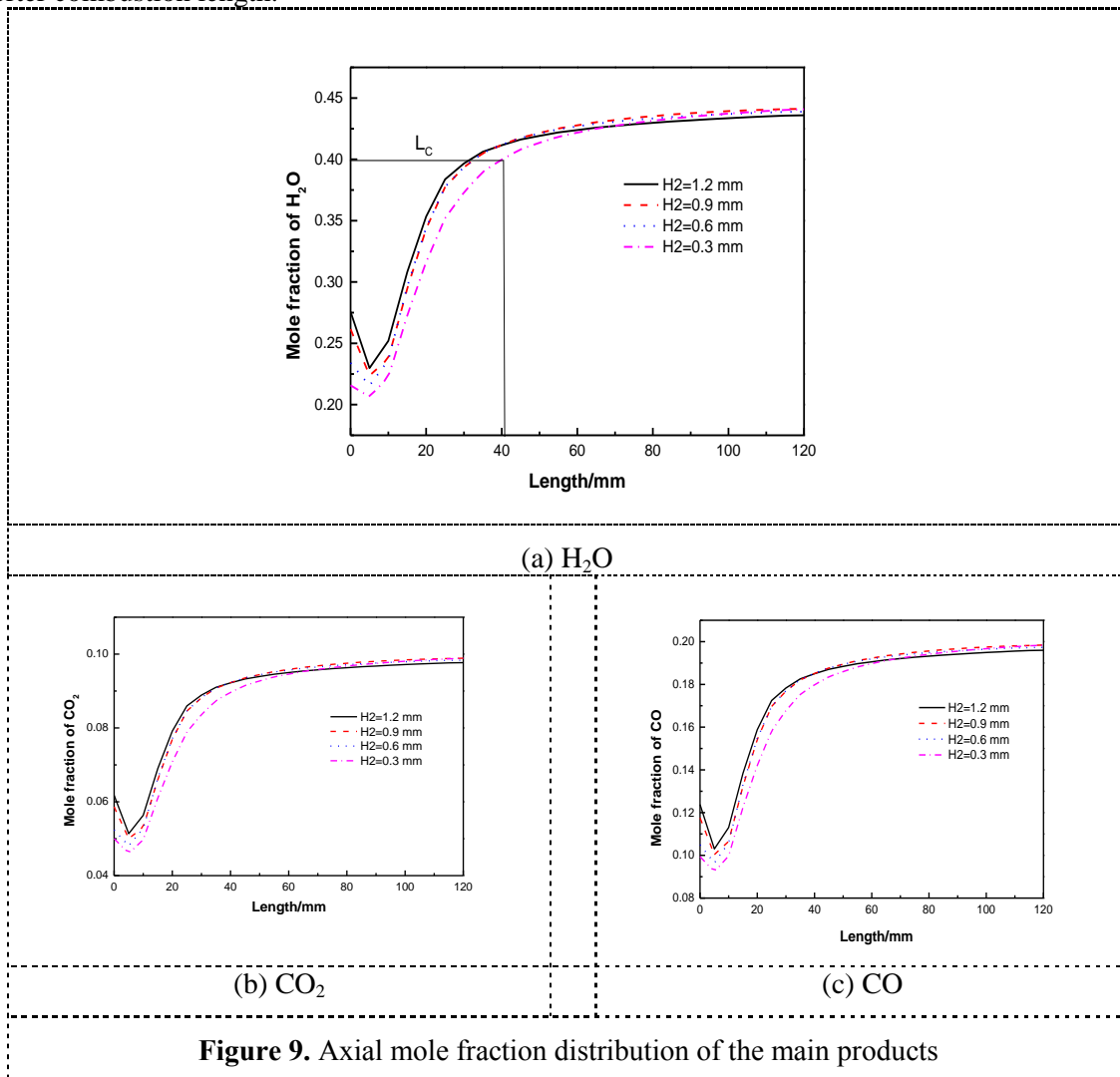


Figure 9. Axial mole fraction distribution of the main products

5. Conclusions

The combustion characteristic of single-element platelet injector with GO₂/GCH₄ as propellant is discussed by numerical method, middle-plate thickness and characteristic chamber length is calculated for improving combustion efficiency. The following conclusions can be obtained: 1) the combustion

distance can be shortened effectively by using platelet injector. Good combustion can be achieved for reasonable characteristic chamber length L^* . Characteristic velocity efficiency can reach above 99% when $L^*=600\text{mm}$. 2) the influence of H_2 on temperature, composition distribution and combustion efficiency of splash injector is not very noticeable. When $H_2=0.6\text{mm}$, the combustion performance can reach the best. In general, this configuration has a better combustion performance, shorter combustion length. 3) these efforts can aid in the optimization of the splash platelet injector in order to achieve the highest mixing characteristic and combustion efficiency. For the later, other key parameters including expending angle, relative thickness, nozzle space and the heat load of the injector faceplate et al. will be studied, and detailed chemical reaction model should be adopted. This works are still going on.

6. Acknowledgments

The authors gratefully acknowledge the financial support of National Science Foundation of China (Grant NO.90916018) and National Science Foundation of Hunan (Grant NO.13JJ2002)

7. References

- [1] Robbers B A, Anderson B J, Hayes W A. et al. Platelet devices-limited only by one's imagination, AIAA 2006-4542, 42nd AIAA/ASME/SAE/ASEE Joint Propulsion Conference & Exhibit, July9-12, 2006, Sacramento, California.
- [2] Philip J. Robinson, Eric M. Veith, Eric A. Hurlbert, et al, 445N (100-lbf) LO₂/LCH₄ reaction control engine technology development for future space vehicles, Acta Astronautica, 66(2010) 836-843.
- [3] Todd Neill, Donald Judd, Eric Veith, Donald Rousar, Practical uses of liquid methane in rocket engine applications, Acta Astronautica, 65(2009) 696-705.
- [4] O. Schwarz, P. Q. Duong, G. Schafer, R. Schomacker, Development of a microstructured reactor for heterogeneously catalyzed gas phase reactions: Part I. Reactor fabrication and catalytic coatings, Chemical Engineering Journal, 145(2009)420-428.
- [5] Liu Hongpeng, Liu Weiqiang, A numerical model for the platelet heat-pipe-cooled leading edge of hypersonic vehicle, Acta Astronautica, 118(2016) 210-217.
- [6] Charles E. Hickox. Characterization of typical platelet injector flow configurations, NASA Report N75-30468.
- [7] H. H Mueggengurg. Platelet injector design and development history. AIAA/SAE/ASME/ASEE 27th Joint Propulsion Cong, 1991.
- [8] Li Junhai, Zeng Peng, Yu Nanjia, Cai Guobiao, Design and experimental research of a gas oxygen/propane small thrust engine, Journal of Aerospace Power, 26(10): 2352-2357, 2011.
- [9] Bassham L B, Labotz R J, Michel P W. Space Shuttle Orbital Maneuvering Engine Platelet Injector Program, NASA Report N76-18231.
- [10] Kahl R C, Labotz R J, Bassham L B, Platelet Injector for Space Shuttle Orbital Maneuvering Engine, AIAA/SAE 10th Propulsion Cong, 1974.
- [11] Lei Fanpei, Zhang Zhenpeng, Yao Mingming et al. Experimental investigation on flow rate and mixing characteristics of splash platelet injector element, Journal of Aerospace Power, 24(6): 1402-1406, 2009.
- [12] Guo Zhihui, Cao Yong, Huang Yong, Spray characteristics of side unlike impinging platelet injector, Journal of Aerospace Power, 20(2): 202-207, 2005.
- [13] Sozer E, Vaidyanathan A, Segal C, et al, Computational assessment of gaseous reacting flows in single element injector, AIAA Paper No.2009-449.
- [14] Lin J, West J S, Williamst R W, CFD code validation of wall heat fluxes for a GO₂/GH₂ single element combustor, AIAA Paper No. 2005-4524.
- [15] Wang Xiaowei, Cai Guobiao, Jin Ping, Scaling of the flowfield in a combustion chamber with a gas-gas injector, 2010 Chinese. Phys. B, 19 019401.

- [16] Conley A, Vaidyanathan A, Segal C, Heat flux measurements for a GO₂/GH₂ single-element, shear injector, *Journal of Spacecraft and Rockets*, 44(3): 633-639, 2007.
- [17] Gao Yushan, Du Zhenggang, Jin Ping, Cai Guobiao, Numerical simulation on the combustion characteristic of shear coaxial GO₂/GCH₄ injector, *Journal of rocket propulsion*, 35(5): 18-23, 2009.
- [18] Botz R J L, Development of the platelet micro-orifice injector, 35th IAF Cong, 1984.